View metadata, citation and similar papers at core.ac.uk

brought to you by CORE

provided by Ulster University's Research Portal

American Journal of Pathology, Vol. 166, No. 2, February 2005
Copyright © American Society for Investigative Pathology

Vascular Biology, Atherosclerosis and Endothelium Biology

Inhibition of Tumor Necrosis Factor-α Improves Physiological Angiogenesis and Reduces Pathological Neovascularization in Ischemic Retinopathy

Tom A. Gardiner,* David S. Gibson,* Tanyth E. de Gooyer,* Vidal F. de la Cruz,† Denise M. McDonald,* and Alan W. Stitt*

From Ophthalmology and Vision Science, Queen's University Belfast, Belfast, Northern Ireland; and Cytokine PharmaSciences, Inc.,† King of Prussia, Pennsylvania*

The present study was undertaken to test whether inhibition of the proangiogenic inflammatory cytokine tumor necrosis factor (TNF)-α can modulate retinal hypoxia and preretinal neovascularization in a murine model of oxygen-induced retinopathy (OIR). OIR was produced in TNF-α−/− and wild-type (WT) control C57B6 neonatal mice by exposure to 75% oxygen between postnatal days 7 and 12 (P7 to P12). Half of each WT litter was treated with the cytokine inhibitor semapimod (formerly known as CNI-1493) (5 mg/kg) by daily intraperitoneal injection from the time of reintroduction to room air at P12 until P17. The extent of preretinal neovascularization and intraretinal revascularization was quantified by image analysis of retinal flat-mounts and retinal hypoxia correlated with vascularization by immunofluorescent localization of the hypoxia-sensitive drug pimonidazole (hypoxyprobe, HP). HP adducts were also characterized by Western analysis and quantified by competitive enzyme-linked immunosorbent assay. TNF-α−/− and WT mice showed a similar sensitivity to hyperoxia-induced retinal ischemia at P12. At P13 some delay in early reperfusion was evident in TNF-α−/− and WT mice treated with semapimod. However, at P17 both these groups had significantly better vascular recovery with less ischemic/hypoxic retina and preretinal neovascularization compared to untreated retinopathy in WT mice. Immunohistochemistry showed deposition of HP in the avascular inner retina but not in areas underlying preretinal neovascularization, indicating that such aberrant vasculature can reduce retinal hypoxia. Inhibition of TNF-α significantly improves vascular recovery within ischemic tissue and reduces pathological neovascularization in OIR. HP provides a useful tool for mapping and quantifying tissue hypoxia in experimental ischemic retinopathy. ***(Am J Pathol 2005, 166:637–644)***

Angiogenesis is associated with two major paradigms of causation: inflammation and hypoxia. Although the central players, such as vascular endothelial growth factor (VEGF), are common to each of these models,[1,2] it is clear that some molecules characteristically associated with angiogenesis in either hypoxia or inflammation may be important to both in certain circumstances. In particular, the roles of the inflammatory cytokines, especially tumor necrosis factor (TNF)-α, interleukin (IL)-1, and IL-8, are emphasized in inflammation-associated angiogenesis[3–7] although their importance in noninflammatory angiogenesis is also becoming evident.[8] There is also considerable evidence that hypoxia-inducible factor, the chief *trans*-acting transcription factor for VEGF may represent an important link between angiogenesis occurring during hypoxia or in inflammation.[9,10] In addition to hypoxia, hypoxia-inducible factor has been shown to be regulated by cytokines, even under normoxic conditions.[11]

Oxygen-induced retinopathy (OIR) in neonatal mice[12] represents a model of hypoxia-driven retinal neovascularization devoid of any obvious inflammatory infiltrate. In this model the mice are exposed to hyperoxia for 5 days between postnatal day 7 (P7) and P12. As vascularization of the murine retina takes place throughout the first 2 weeks of postnatal development, the retinal vasculature

Supported by the Wellcome Trust and the Research and Development Office Northern Ireland.

T.A.G. and D.S.G. contributed equally to this work.

Accepted for publication October 21, 2004.

Address reprint requests to Professor A.W. Stitt, Ophthalmology and Vision Science, Queen's University Belfast, Royal Victoria Hospital, Grosvenor Road, Belfast, BT12 6BA, Northern Ireland. E-mail: a.stitt@qub.ac.uk.

at P7 is immature with only the primary inner vascular plexus in place. The hyperoxia causes vaso-obliteration of the central retinal capillary beds by two recognized mechanisms: it rapidly down-regulates VEGF production by the retinal parenchyma and renders the immature capillaries vulnerable to apoptosis[13–15] while simultaneously inducing an oxidative insult mediated by endogenous nitric oxide production.[16] It is also likely that the oxidative insult is augmented by up-regulation of pigment epithelium-derived factor, which has been shown to be anti-angiogenic and proapoptotic for activated vascular endothelial cells.[17–19] After return to room air at P12 the avascular regions of the central retina are rendered hypoxic with an associated liberation of angiogenic growth factors.[20] Subsequently, retinal angiogenesis occurs in two separate locations. Firstly, there is a variable revascularization of the ischemic central capillary beds. Secondly, preretinal neovascularization results in the proliferation of new vessels on the surface of the retina, within the vitreous body. The preretinal vessels are derived from viable vasculature at the margins of the ischemic central retina, from the perfused periphery and the optic disk. Neovascular complexes tend to overlie persistently ischemic areas of the central retina and are less developed in quadrants where intraretinal revascularization has occurred. This report describes how alteration of the cytokine profile during the hypoxic/angiogenic phase of OIR by semapimod (formerly known as CNI-1493), a translational inhibitor of TNF-α,[21,22] or by ablation of the TNF-α gene may alter the balance of hypoxia and angiogenesis within the intraretinal and preretinal compartments of the eye. It also indicates fundamental differences in the needs of angiogenic vessels proliferating within differing extracellular environments.

Materials and Methods

Experimental Design

OIR was induced in C57/BL6 wild-type (WT) and TNF-$\alpha-/-$ mice[23] (on a C57/BL6 genetic background) (Banton & Kingman, Hull, UK) as described by Smith and colleagues.[12] Briefly, neonatal mice and their nursing dams were exposed to 75% oxygen (PRO-OX 110 chamber oxygen controller used; Biospherix Ltd., Redfield, NY) between postnatal day 7 (P7) and P12 producing vaso-obliteration and cessation of vascular development in the capillary beds of the central retina. Return of the animals to room air at P12 renders the central retina ischemic and hypoxic, and results in preretinal neovascularization between P15 and P21 with maximal neovascularization at P17. In each experiment two P12 animals received an intravenous injection of fluorescein-dextran (2×10^6 MW) (Sigma-Aldrich Ltd., Gillingham, UK) and were sacrificed immediately on return to room air. Retinal flat-mount angiograms were then prepared to confirm consistent vaso-obliteration of the central capillary beds. As the C57/BL6 dams showed inconsistent care and nutrition of the pups when returned to room air, at P12 all C57/BL6 and TNF-$\alpha-/-$ pups were cross-fostered to nursing Swiss dams that had not been exposed to hyperoxia.

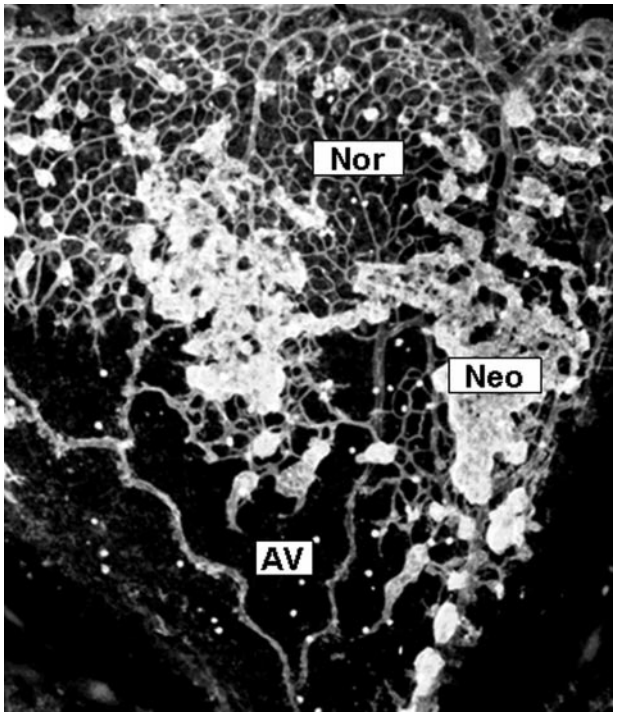

Figure 1. Grading of microvascular configuration in OIR. The retinal microvasculature was localized and identified in retinal flat-mounts using confocal scanning laser microscopy. This representative image shows area of normal intraretinal capillaries (Nor), regions of avascular retina (ischemia, AV), and distinct, hyperfluorescent regions of preretinal neovascularization (Neo).

Assessment of Preretinal Neovascularization and Intraretinal Angiogenesis

Multiple timed matings were prepared for both WT and TNF-$\alpha-/-$ mice and subjected to OIR. WT neonates were divided into two equal groups; one being treated with semapimod (Cytokine PharmaSciences, Inc., King of Prussia, PA) (5 mg/kg) by daily intraperitoneal injection between P12 and P17 and the other OIR control group treated with vehicle (2.5% mannitol in water) alone. In all cases there was a minimum of 10 pups/group. At P17, semapimod-treated mice, controls, and TNF-$\alpha-/-$ mice previously exposed to hyperoxia were terminally anesthetized and perfused with fluorescein-dextran via the left ventricle. On enucleation, both eyes were fixed in 4% paraformaldehyde for 4 hours at 4°C, one for subsequent wax histology and the other for flat-mount angiography or fluorescent lectin histochemical staining with *Griffonia simplicifolia* isolectin B4 (Figure 1). Each experiment was conducted three times.

Configuration of the microvascular tree was assessed in retinal flat-mounts using an image analysis-based evaluation of 1) avascular regions, 2) areas of intraretinal perfusion, and 3) preretinal neovascularization (Figure 1). Whole retinas fluorescently stained with biotin-labeled isolectin B4 and Alexa-488 streptavidin (described below and illustrated in Figure 1) were analyzed in a blinded

manner by a skilled investigator using the Lucia image analysis system (supplied by Nikon, UK). The three categories described above were outlined and quantified in each quadrant of the retina as fractions of the total area of retina analyzed. Images were acquired using a Nikon Eclipse E400 fluorescence microscope at ×40 magnification using a Nikon DXM 1200 digital camera via Nikon image-capture software (at 600 dpi resolution) and stored as TIFF files. Five separate fields were required to cover the four retinal quadrants and the optic disk within each flat-mount. The files were opened in LUCIA G (version 4.71) image analysis software (obtained from Nikon), which allows pixel calibration in μm for each microscope lens magnification. A binary overlay was prepared from each image and total retinal areas, in μm^2, were assessed by interactively drawing a line around the edge of individual retinal quadrants. Ischemic (nonvascularized) or neovascularized areas were similarly outlined and their area fractions of the total retinal area in each image calculated by the software. Often the greater fluorescent intensity of the neovascular tissue could be outlined and assessed completely automatically by setting a suitable threshold of image intensity for capture in the binary image, sufficient to outline only the neovascular tufts. Statistical analysis was performed using a one-way analysis of variance and a Tukey-Kramer post test for multiple comparisons; a P value ≤ 0.05 was considered significant.

Sodium Dodecyl Sulfate-Polyacrylamide Gel Electrophoresis and Western Blotting

In a parallel experiment semapimod-treated mice and OIR controls were sacrificed at P13, P15, or P17 and the retinas immediately removed for Western analysis. The disrupted tissue samples of neural retina from each group of animals ($n = 8$) were pooled, centrifuged at 15,000 rpm for 15 minutes to remove cell debris, and the soluble protein extract in the supernatant was harvested for subsequent sodium dodecyl sulfate-polyacrylamide gel electrophoresis. The concentration of protein in the samples was estimated using a BCA protein assay kit (Pierce, Rockford, IL) and sodium dodecyl sulfate-polyacrylamide gel electrophoresis was performed under both denaturing and nondenaturing conditions. After transfer to a nitrocellulose membrane (Bio-Rad, Hercules, CA) and blocking with 5% nonfat milk the blot was probed with anti-TNF-α goat polyclonal antibody (Santa Cruz Biotechnology Inc., Santa Cruz, CA), iNOS rabbit polyclonal antibody (AbCam, Cambridge, UK), or β-actin rabbit polyclonal antibody (AbCam) in Tris-buffered saline-Tween for 2 hours. After extensive washing in Tris-buffered saline-Tween an anti-goat secondary antibody-horseradish peroxidase conjugate (DAKO, AS, Glostrup, Denmark) was added to the membrane at a dilution of 1:2500 for 45 minutes. As a loading control, β-actin was probed with a 1:5000 dilution of a monoclonal antibody (mAb) (Sigma-Aldrich Ltd.) for 1 hour, washed as before, and detected with an appropriate second Ab-horseradish peroxidase conjugate (Santa Cruz Biotechnology Inc.).

Immunoreactivity was detected with Supersignal West Pico chemiluminescent substrate (Pierce) on Hyperfilm (Amersham Biosciences UK Ltd., Chalfont St. Giles, UK). Band densitometry was performed using LabWorks v4.08 software on images acquired by AutoChemi system (charge-coupled device camera and autorad transillumination) (both from UVP Inc., Upland, CA). Statistical analysis was conducted using a one-way analysis of variance and data were considered significant at 95% ($P < 0.05$).

Determination of Retinal Hypoxia

Treatment with Hypoxyprobe (HP) Bio-Reductive Drug

For determination of retina hypoxia, further groups at P13 and P17 ($n = 8$) of hyperoxia-exposed mice (WT and TNF-$\alpha-/-$) received an intraperitoneal injection of the bio-reductive drug pimonidazole[24] (HP; Chemicon Europe Ltd., Chandlers Ford, UK) at 60 mg/kg 3 hours before sacrifice to assess retinal hypoxia in semapimod-treated WT and TNF-$\alpha-/-$ animals compared to OIR controls.

HP Immunolocalization

For this, one eye from each animal was fixed in 4% paraformaldehyde for 4 hours and then washed extensively throughout a 4-hour period after which the anterior segment lens complexes were removed and the posterior eye cups relaxed by placing four radial cuts from the retinal periphery to points within 1 mm from the optic disk. The specimens were then given an overnight soak in 96-well plates at 4°C in phosphate-buffered saline (PBS) containing 0.5% Triton X-100 to permeabilize the tissue, and 5% normal goat serum (Sigma-Aldrich Ltd.) to block nonspecific binding of the primary antibody. For visualization of the HP-protein adducts an anti-HP mouse monoclonal antibody (HP-mAb; Chemicon Europe Ltd.) or a rabbit polyclonal antibody (gift from Dr. James A. Raleigh, University of North Carolina School of Medicine, Chapel Hill, NC) were used at a dilution of 1:100 for 4 hours at 37°C and 100% humidity. Each immunoreagent incubation was followed by extensive washing in the permeabilization buffer (8× changes) throughout a further 4 hours at 37°C and an additional block with 5% normal goat serum for 2 hours at 37°C. A 1:500 dilution of a goat anti-mouse polyclonal antibody labeled with Alexa-488 (Molecular Probes Europe BV, Leiden, The Netherlands) was used for secondary detection; the staining time and subsequent washing were as used for the primary antibody. Both retinas of two OIR mice were used for immunocytochemical controls: two were stained with the second antibody only and two with 5% mouse serum (Vector Laboratories Ltd., Peterborough, UK) in place of the primary antibody. If nuclear staining was required, retinas were incubated in 5 nmol/L propidium iodide in permeabilization buffer for 10 minutes at 37°C.

In nonfluorescein-dextran-perfused eyes the retinal vasculature was visualized by reaction with biotinylated

isolectin B4 from *G. simplicifolia* (Sigma-Aldrich Ltd.) at 50 ng/ml followed by streptavidin-Alexa 568 (Molecular Probes Europe BV). Retinal flat-mounts were washed extensively and mounted in Vectasheild (Vector Laboratories Ltd.). Images were acquired using an Olympus BX60 fluorescence microscope (Olympus UK Ltd., London, UK) fitted with a MicroRadiance confocal-scanning laser microscope (Bio-Rad).

Quantification of HP

Unfixed neural retina of WT (semapimod-treated and untreated) and TNF-$\alpha-/-$ mice ($n = 6$) were dissected and subjected to ultrasonic disruption in RIPA buffer. For quantification of HP-protein binding, retinal samples from P13 and P17 mice were prepared for a HP competitive enzyme-linked immunosorbent assay (ELISA) methodology. Briefly, 100 μl of sample or standard in duplicate were serially diluted in PBS/5% Tween 20 in a 96-well polystyrene assay plate (Corning Inc., Corning, NY) and incubated with 25 μl of rabbit polyclonal antibody against HP (1:3300 in PBS/5% Tween; kindly donated by Dr. James A. Raleigh, University of North Carolina School of Medicine, Chapel Hill, NC) for 1 hour at 37°C. The contents of each well was then transferred to NUNC C96 Maxisorp plates that had been precoated with solid phase antigen (1:5000 in carbonate buffer, pH 9.6) overnight at 4°C and blocked with 1% gelatin for 1 hour. The competition between solid phase and soluble antigens proceeded for 1 hour at 37°C, after which the wells were washed 4 × 5minutes with PBS/5% Tween, and 100 μl of 1:2000 alkaline-phosphatase goat anti-rabbit IgG (Sigma-Aldrich) was added to each well. Plates were then washed 4 × 5minutes with PBS/5% Tween, and 100 μl of 1 mg/ml of the alkaline-phosphatase substrate, 4-nitrophenyl phosphate disodium salt hexahydrate (Sigma-Aldrich) dissolved in 10% diethanolamine buffer (pH 9.6) was added to each well. The color development of the subsequent reaction was measured at 405 nm every 5 minutes for 2 hours on a Safire microplate reader (Tecan Instruments) and reaction kinetics analyzed using Magellan 3 software. Sample HP-1 binding was determined by comparison to a Lineweaver-Burk enzyme kinetic standard curve, and is expressed as a proportion of sample protein concentration. The solid-phase antigen used in this assay was HP, which had been reductively bound to bovine serum albumin.[25] Statistical analysis was conducted using the Student's *t*-test and a P value <0.05 was considered significant.

Results

Western analysis for retinal TNF-α expression demonstrated a reduction in non-OIR mice from P13 to P17 (Figure 2). On densitometric quantification of retinal extracts from OIR-controls, there was a significant increase in TNF-α expression at P15 and P17 compared to the P13 time point ($P < 0.05$) (Figure 2). In semapimod-treated mice subjected to OIR, there was a significant reduction

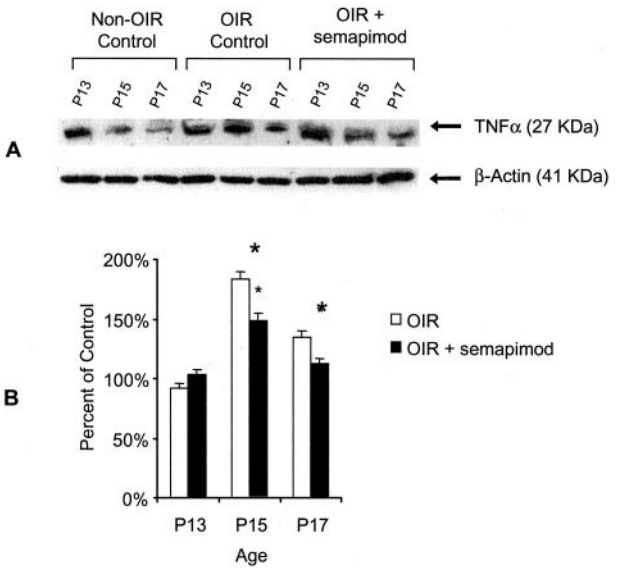

Figure 2. Semapimod inhibits TNF-α in murine retina. **A:** Representative Western blot analysis of TNF-α and β-actin in murine retina from nonhyperoxia-exposed mice, OIR mice, and OIR mice treated with semapimod. Data are shown for retinal extracts from P13, P15, and P17 time periods. **B:** Densitometric analysis of TNF-α Western blot. Data represent the mean ± SD for $n = 3$ independent experiments. Data are expressed as percentage of control (room air only) mice. *, Significantly different from OIR control ($P < 0.05$).

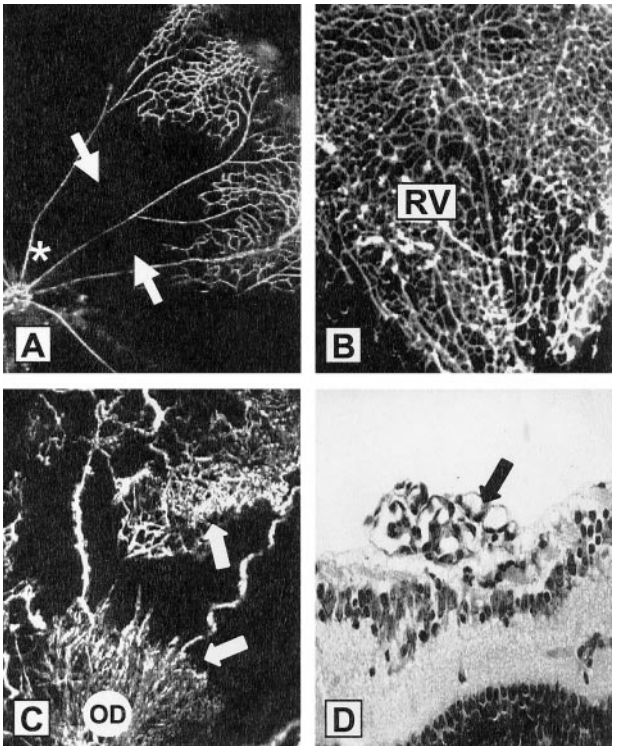

Figure 3. OIR-induced retinal ischemia: promotion of intraretinal revascularization by TNF-α inhibition. FITC-dextran angiograms of retinal quadrants from OIR control animals show a complete closure of the central retinal capillary beds (**arrows**) at P12 (**A**) (optic disk is indicated by *). **B:** At P17 semapimod-treated OIR mice show evidence of intraretinal revascularization (RV). **C:** WT OIR (control) mice at P17 show areas of preretinal neovascularization (**arrows**), both at the peripheral retina and optic disk (OD). **D:** In H&E-stained sections there are clear neovascular complexes on the retinal surface (**arrow**).

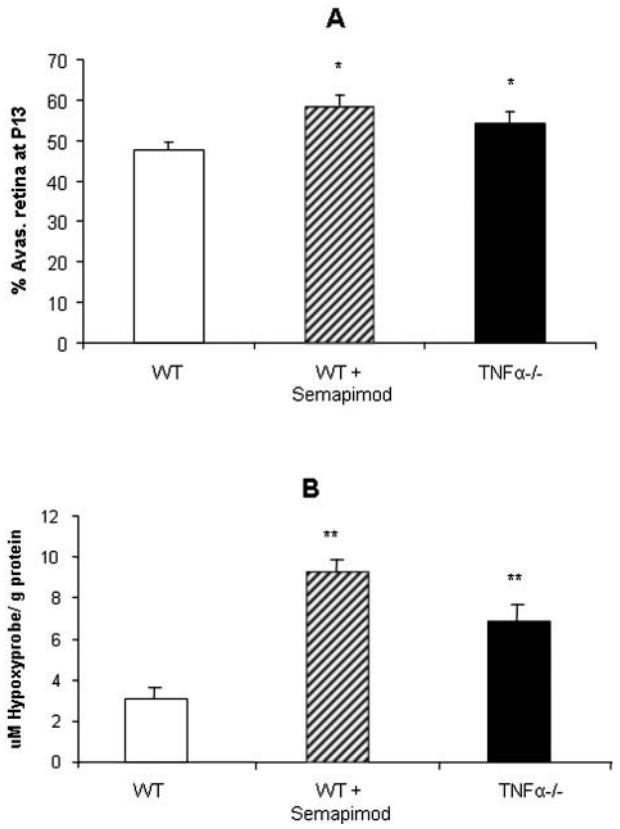

Figure 4. A: TNF-α modulates hyperoxia-induced retinal vascular closure. The areas of avascular retina were quantified in retinal flat-mounts at P13. When WT OIR mice were treated with semapimod there was an increase in the area of avascular retina in comparison to OIR WT controls. This pattern of avascular retina was also evident in TNF-$\alpha-/-$ mice subjected to OIR. Data are the mean ± SD for $n = 3$ independent experiments (*, $P < 0.05$). **B:** Retinal hypoxia is increased with semapimod or absence of TNF-α. Competitive HP ELISA demonstrates increased HP immunoreactivity in retinal lysates from P13 mice for both semapimod-treated mice and TNF-$\alpha-/-$ mice. Data are expressed as the mean concentration per g of total protein (μmol/L/g) ± SD for $n = 6$ (**, $P < 0.01$; $n = 3$ independent experiments).

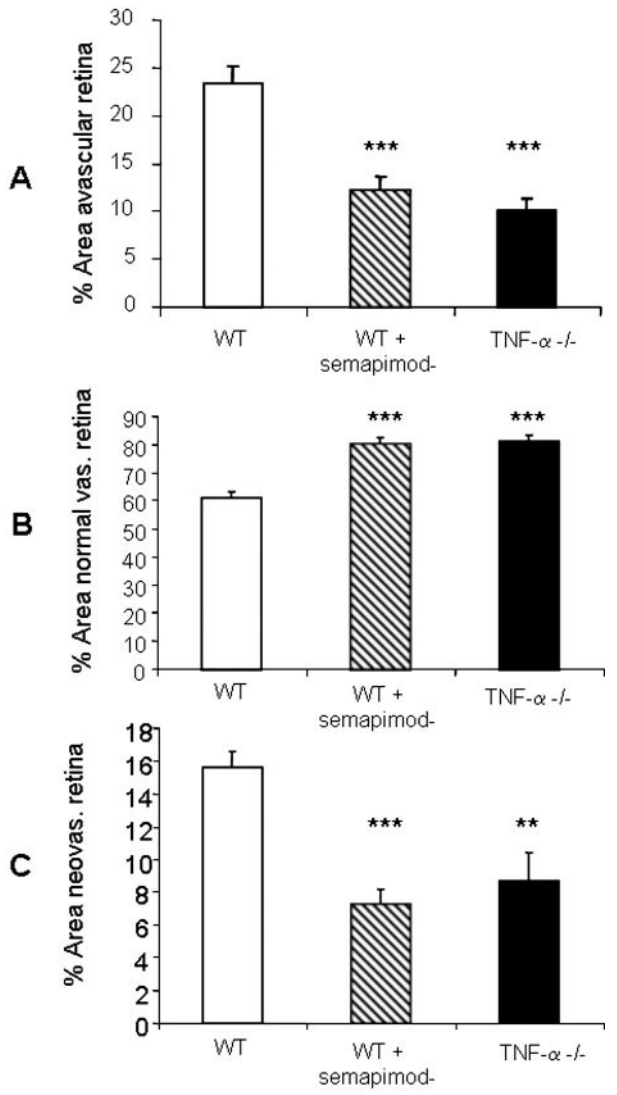

Figure 5. TNF-α inhibition or deletion reduces retinal neovascularization with concomitant reduction of ischemia and promotion of normal retinal vascularization. Quantitative analysis was performed on the entire retinal microvasculature in flat-mounts at P17. Semapimod treatment and absence of TNF-α resulted in a significant decrease in retinal ischemia (**A**), an increase in normal (intraretinal) vascularization (**B**), and a decrease in preretinal neovascularization (**C**) when compared to WT controls. Data are the mean ± SD for $n = 3$ independent experiments. **, $P < 0.01$; ***, $P < 0.001$.

in retinal TNF-α expression at both P15 and P17 when compared to OIR controls (~50%; $P < 0.05$) (Figure 2).

When neonatal mice were returned to room air after hyperoxia (P12) the established closure and nondevelopment of the central capillary beds rendered the central retina ischemic/hypoxic (Figure 3A). A further 5 days in room air produced some intraretinal vascular recovery with revascularization from the perfused retinal periphery, especially in semapimod-treated or TNF-$\alpha-/-$ mice (Figure 3B). Neovascular complexes originating at the perfused periphery and optic disk were seen to invade the vitreous body and proliferate on the retinal surface overlying the hypoxic neuropile (Figure 3, C and D). At P13, which represents a full 24 hours of ischemic hypoxia in the central retina, treatment with semapimod caused an increase in the area of avascular/ischemic retina in comparison to OIR controls ($P < 0.01$) (Figure 4A); a similar trend was noted in the TNF-$\alpha-/-$ mice and reflected in the overall level of retinal hypoxia as quantified by competitive ELISA analysis of HP adducts (Figure 4B). However, by P17 the situation was reversed. Compared to OIR controls at P17, there was a significant decrease in area of avascular (ischemic) retina in both TNF-$\alpha-/-$ mice and WT animals treated with semapimod ($P < 0.001$) (Figure 5A). This was accompanied by a corresponding and significant increase ($P < 0.001$) in intraretinal vascularization (normal vascularization, Figure 5B) and a decrease in preretinal neovascularization ($P < 0.01$ to 0.001) (Figure 5C) in semapimod-treated and TNF-$\alpha-/-$ mice when compared to WT OIR control animals. In all of the retinal vascular parameters analyzed, there was no significant difference between semapimod treatment and deletion of TNF-α (Figure 5). ELISA quantification of HP adducts at P17 proved unreliable because some HP deposits in the vascular endothelial cells during postmortem hypoxia and the large increase in the overall quantity of retinal vessels at P17 compared to P13 meant that this discrepancy became significant. Interpretation of HP ELISA data at P17 was further complicated by the

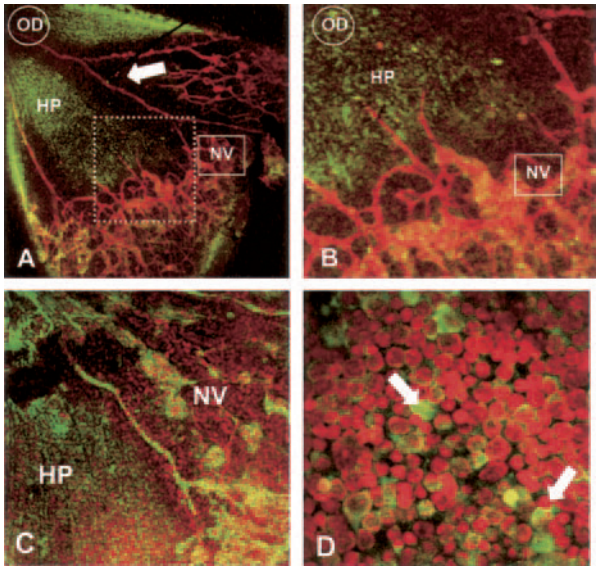

Figure 6. HP is deposited at sites of retinal hypoxia during OIR. **A:** At P13 HP deposition is evident (represented by green fluorescence) in the avascular central retina but not in the perfused peripheral retina. Vessels were visualized with isolectin B_4 (red fluorescence); optic disk (OD) and neovascularization is apparent at the periphery (NV), but not adjacent to the major retinal arteries (**arrow**). **B:** On higher magnification of **A** (represented by **dashed inset**) fronds of new vessels (NV) are observed but there is little HP in the underlying retinal neuropile. **C:** At P17, no HP is evident in the areas underlying neovascularization (NV). **D:** High magnification of P13 retinal flat-mounts using PI as a nuclear stain reveals high levels of HP immunoreactivity in neurons of the ganglion cell layer (**arrows**) within nonperfused central retina, remote from traversing arterioles. Original magnifications: ×100 (**A**, **C**); ×200 (**B**, **D**).

fact, as noted below in immunofluorescent staining, that the preretinal neovascular complexes provided sufficient oxygenation to prevent the reduction of HP in the underlying neural retina.

Immunofluorescent localization of the hypoxia marker pimonidazole (HP) showed deposition of protein adducts within the nonperfused central retina distal from the traversing major blood vessels (Figure 6, A and B). Interestingly, no HP staining was detected in nonperfused retina underlying preretinal neovascularization complexes (Figure 6C) indicating that the underlying inner retina was receiving significant oxygenation from the overlying neovascularization to prevent the reductive metabolism of HP and deposition of stainable drug-protein adducts.

HP was deposited predominantly within the cytoplasm of neurons in the ganglion cell layer (Figure 6D) reflecting both their metabolic activity and distal location to the nearest source of oxygen in the choroid; the stained cells probably included both ganglion and displaced amacrine cells. Positive staining for HP was also detected in some horizontally orientated cell processes in the inner plexiform layer but not in the outer retina beyond the inner nuclear layer (data not shown). It was of interest that HP did not appear to deposit in the retinal astrocytes, located between the ganglion cell layer and the internal limiting membrane. Double immunostaining of the astrocytes for HP and glial fibrillary acidic protein revealed no co-localization (data not shown). Positive staining of the blood vessels by the HP monoclonal Ab was initially thought to be because of detection of mouse IgG in the blood column by the secondary Ab as it was also present in second Ab only controls, however, subsequent staining with a rabbit polyclonal Ab for HP also showed positive, although reduced, staining in the vessels, confirming reductive metabolism of HP because of postmortem hypoxia.

Discussion

Neovascular retinopathies collectively represent a major cause of blindness in developed countries and are characterized by hypoxia-driven angiogenesis in which new blood vessels escape the confines of the retina and grow on the retinal surface. It is not known why such new vessels tend to proliferate outside the retina in preference to infiltration of the hypoxic tissue. However, it is increasingly clear that this situation is open to pharmacological manipulations that either inhibit endogenous anti-angiogenic factors within the ischemic tissue,[26] or actively enhance proangiogenic processes such as cell attachment.[27] Such treatments have the potential to encourage therapeutic angiogenesis within the ischemic retina, reduce tissue hypoxia, and quench the persistent stimulus for further pathological intravitreal neovascularization.

TNF-α has been shown to be anti-angiogenic *in vitro*[28] but proangiogenic *in vivo*,[4,29] possibly through stimulation of VEGF induction[30] and enhanced expression of cell-associated proteases.[8,31,32] However, there is little published evidence concerning the role of cytokines in the context of hypoxia-driven angiogenesis in ischemic retinopathy. In the present study we showed that, after an initial delay, effective absence of TNF-α (by gene ablation or pharmacological inhibition), facilitated revascularization of the ischemic central retina, with a concomitant reduction in neovascular invasion of the vitreous body during OIR. The data showed good correlation of ischemia and hypoxia at P13, as expressed by the relative areas of avascular retina and deposition of the hypoxia-sensitive drug pimonidazole (HP). Also, immunofluorescent staining of HP adducts confirmed that the avascular regions of inner retina were invariably hypoxic. In the context of the neural retina this finding has some importance: The possibility of oxygen diffusion from the underlying choroid and adjacent ciliary circulation means that the terms avascular and ischemic are not necessarily synonymous when applied to the retina. Nitroimidazoles are excellent indicators of hypoxia with sufficient sensitivity to demonstrate even physiological oxygen gradients.[33] As deposition of HP becomes significant at pO_2 levels $<$10mmHg,[34] an oxygen tension not significantly lower than what is considered physiological at the outer plexiform layer in normal retina,[35] it is reasonable to conclude that the neovascular complexes on the retinal surface were able to oxygenate the underlying retina to at least such a degree. This finding is of interest in that neovascular complexes at the retinal surface are likely to reduce the expression of vasogenic growth factors by the underlying parenchyma. The production of VEGF in particular is mediated by hypoxia-inducible factor, the expression and stabilization of which increases in inverse

proportion to tissue oxygen levels[36] and it is clear that increased perfusion of the retinal neuropile in the later stages of OIR (P17 to P21), either by intraretinal or intravitreal vascularization, is likely to reduce hypoxia, and associated VEGF expression. Such a sequence thereby reduces the stimulus for neovascularization with resolution of the angiogenic response. A similar natural history ensues in untreated ischemic retinopathy in human disease but in that situation the misplaced neovascular response and associated scar tissue lead to tractional retinal detachment and vitreous hemorrhage.

It is not clear why TNF-α inhibition should impair reperfusion of the ischemic retina in the early hypoxic stage of OIR yet enhance it in the later neovascular phase of the condition. However, the greater level of inner retinal ischemia in semapimod-treated WT and TNF-$\alpha-/-$ mice at P13 suggests that initial hypoxia-driven vasodilatation by surviving retinal vessels may be dependent on cytokines or associated inflammatory mediators such as the vasodilator nitric oxide. Despite such delay in the immediate response of the retinal vasculature to hypoxia, TNF-α blockade served to facilitate intraretinal angiogenesis and recovery of the ischemic retina; this was associated with a concomitant reduction of intravitreal neovascularization in TNF-$\alpha-/-$ and semapimod-treated WT mice at P17. Such a switch from intravitreal neovascularization to intraretinal angiogenesis has been previously described by Sennlaub and colleagues[26] in inducible nitric oxide synthase (iNOS) knockout mice and because TNF-α and iNOS are co-expressed in a host of inflammatory situations it is possible that both these phenomena are linked. Although angiogenesis in the model of ischemic retinopathy used in this study is driven by hypoxia-mediated expression of VEGF[12,15,37] in the absence of any significant inflammatory infiltrate, it is clear that the nature of the angiogenic response is under the control of inflammatory mediators[38–42] and that TNF-α has an important role.

This study has correlated vascular recovery and neovascularization with tissue hypoxia in ischemic retinopathy and shown that preretinal neovascular complexes at the retinal surface effectively oxygenate the underlying retinal neuropile. The data presented also shows that inhibition/deletion of TNF-α facilitates physiological angiogenesis within the ischemic retina with a concomitant reduction in pathological neovascularization of the vitreous body. This emphasizes the interdependence of angiogenesis within these two contiguous but radically different tissue environments in the pathogenesis of neovascular retinopathies and the need to account for both when evaluating new therapeutic strategies for the treatment of retinal neovascularization. The findings further substantiate the possibility of redirection of the angiogenic stimulus for therapeutic angiogenesis in the treatment of ischemic retinopathies.

Acknowledgments

We thank Mr. Matthew Owens for technical expertise and Dr. James A. Raleigh (University of North Carolina School of Medicine, Chapel Hill, NC) for the generous gifts of HP polyclonal antibody and HP-BSA.

References

1. McCourt M, Wang JH, Sookhai S, Redmond HP: Proinflammatory mediators stimulate neutrophil-directed angiogenesis. Arch Surg 1999, 134:1322–1331
2. Semenza GL: Regulation of hypoxia-induced angiogenesis: a chaperone escorts VEGF to the dance. J Clin Invest 2001, 108:39–40
3. Leibovich SJ, Polverini PJ, Shepard HM, Wiseman DM, Shively V, Nuseir N: Macrophage-induced angiogenesis is mediated by tumour necrosis factor-alpha. Nature 1987, 329:630–632
4. Frater-Schroder M, Risau W, Hallmann R, Gautschi P, Bohlen P: Tumor necrosis factor type alpha, a potent inhibitor of endothelial cell growth in vitro, is angiogenic in vivo. Proc Natl Acad Sci USA 1987, 84:5277–5281
5. BenEzra D, Hemo I, Maftzir G: In vivo angiogenic activity of interleukins. Arch Ophthalmol 1990, 108:573–576
6. Norrby K: Interleukin-1-alpha and de novo mammalian angiogenesis. Microvasc Res 1997, 54:58–64
7. Koch AE, Polverini PJ, Kunkel SL, Harlow LA, DiPietro LA, Elner VM, Elner SG, Strieter RM: Interleukin-8 as a macrophage-derived mediator of angiogenesis. Science 1992, 258:1798–1801
8. Koolwijk P, van Erck MG, de Vree WJ, Vermeer MA, Weich HA, Hanemaaijer R, van Hinsbergh VW: Cooperative effect of TNFalpha, bFGF, and VEGF on the formation of tubular structures of human microvascular endothelial cells in a fibrin matrix. Role of urokinase activity. J Cell Biol 1996, 132:1177–1188
9. Stiehl DP, Jelkmann W, Wenger RH, Hellwig-Burgel T: Normoxic induction of the hypoxia-inducible factor 1alpha by insulin and interleukin-1beta involves the phosphatidylinositol 3-kinase pathway. FEBS Lett 2002, 512:157–162
10. Sandau KB, Zhou J, Kietzmann T, Brune B: Regulation of the hypoxia-inducible factor 1alpha by the inflammatory mediators nitric oxide and tumor necrosis factor-alpha in contrast to desferroxamine and phenylarsine oxide. J Biol Chem 2001, 276:39805–39811
11. Hellwig-Burgel T, Rutkowski K, Metzen E, Fandrey J, Jelkmann W: Interleukin-1beta and tumor necrosis factor-alpha stimulate DNA binding of hypoxia-inducible factor-1. Blood 1999, 94:1561–1567
12. Smith LE, Wesolowski E, McLellan A, Kostyk SK, D'Amato R, Sullivan R, D'Amore PA: Oxygen-induced retinopathy in the mouse. Invest Ophthalmol Vis Sci 1994, 35:101–111
13. Stone J, Itin A, Alon T, Pe'er J, Gnessin H, Chan-Ling T, Keshet E: Development of retinal vasculature is mediated by hypoxia-induced vascular endothelial growth factor (VEGF) expression by neuroglia. J Neurosci 1995, 15:4738–4747
14. Alon T, Hemo I, Itin A, Pe'er J, Stone J, Keshet E: Vascular endothelial growth factor acts as a survival factor for newly formed retinal vessels and has implications for retinopathy of prematurity. Nat Med 1995, 1:1024–1028
15. Pierce EA, Foley ED, Smith LE: Regulation of vascular endothelial growth factor by oxygen in a model of retinopathy of prematurity. Arch Ophthalmol 1996, 114:1219–1228
16. Brooks SE, Gu X, Samuel S, Marcus DM, Bartoli M, Huang PL, Caldwell RB: Reduced severity of oxygen-induced retinopathy in eNOS-deficient mice. Invest Ophthalmol Vis Sci 2001, 42:222–228
17. Stellmach V, Crawford SE, Zhou W, Bouck N: Prevention of ischemia-induced retinopathy by the natural ocular antiangiogenic agent pigment epithelium-derived factor. Proc Natl Acad Sci USA 2001, 98: 2593–2597
18. Duh EJ, Yang HS, Suzuma I, Miyagi M, Youngman E, Mori K, Katai M, Yan L, Suzuma K, West K, Davarya S, Tong P, Gehlbach P, Pearlman J, Crabb JW, Aiello LP, Campochiaro PA, Zack DJ: Pigment epithelium-derived factor suppresses ischemia-induced retinal neovascularization and VEGF-induced migration and growth. Invest Ophthalmol Vis Sci 2002, 43:821–829
19. Dawson DW, Volpert OV, Gillis P, Crawford SE, Xu H, Benedict W, Bouck NP: Pigment epithelium-derived factor: a potent inhibitor of angiogenesis. Science 1999, 285:245–248
20. Simpson DA, Murphy GM, Bhaduri T, Gardiner TA, Archer DB, Stitt AW: Expression of the VEGF gene family during retinal vaso-obliter-

ation and hypoxia. Biochem Biophys Res Commun 1999, 262:333–340
21. Bianchi M, Bloom O, Raabe T, Cohen PS, Chesney J, Sherry B, Schmidtmayerova H, Calandra T, Zhang X, Bukrinsky M, Ulrich P, Cerami A, Tracey KJ: Suppression of proinflammatory cytokines in monocytes by a tetravalent guanylhydrazone. J Exp Med 1996, 183: 927–936
22. Cohen PS, Nakshatri H, Dennis J, Caragine T, Bianchi M, Cerami A, Tracey KJ: CNI-1493 inhibits monocyte/macrophage tumor necrosis factor by suppression of translation efficiency. Proc Natl Acad Sci USA 1996, 93:3967–3971
23. Korner H, Cook M, Riminton DS, Lemckert FA, Hoek RM, Ledermann B, Kontgen F, Fazekas de St Groth B, Sedgwick JD: Distinct roles for lymphotoxin-alpha and tumor necrosis factor in organogenesis and spatial organization of lymphoid tissue. Eur J Immunol 1997, 27: 2600–2609
24. Arteel GE, Thurman RG, Yates JM, Raleigh JA: Evidence that hypoxia markers detect oxygen gradients in liver: pimonidazole and retrograde perfusion of rat liver. Br J Cancer 1995, 72:889–895
25. Raleigh JA, La Dine JK, Cline JM, Thrall DE: An enzyme-linked immunosorbent assay for hypoxia marker binding in tumours. Br J Cancer 1994, 69:66–71
26. Sennlaub F, Courtois Y, Goureau O: Inducible nitric oxide synthase mediates the change from retinal to vitreal neovascularization in ischemic retinopathy. J Clin Invest 2001, 107:717–725
27. Gebarowska D, Stitt AW, Gardiner TA, Harriott P, Greer B, Nelson J: Synthetic peptides interacting with the 67-kd laminin receptor can reduce retinal ischemia and inhibit hypoxia-induced retinal neovascularization. Am J Pathol 2002, 160:307–313
28. Sato N, Fukuda K, Nariuchi H, Sagara N: Tumor necrosis factor inhibiting angiogenesis in vitro. J Natl Cancer Inst 1987, 79:1383–1391
29. Leibovich SJ, Polverini PJ, Shepard HM, Wiseman DM, Shively V, Nuseir N: Macrophage-induced angiogenesis is mediated by tumour necrosis factor-alpha. Nature 1987, 329:630–632
30. Ryuto M, Ono M, Izumi H, Yoshida S, Weich HA, Kohno K, Kuwano M: Induction of vascular endothelial growth factor by tumor necrosis factor alpha in human glioma cells. Possible roles of SP-1. J Biol Chem 1996, 271:28220–28228
31. van Hinsbergh VW, van den Berg EA, Fiers W, Dooijewaard G: Tumor necrosis factor induces the production of urokinase-type plasminogen activator by human endothelial cells. Blood 1990, 75:1991–1998
32. Hanemaaijer R, Koolwijk P, le Clercq L, de Vree WJ, van Hinsbergh VW: Regulation of matrix metalloproteinase expression in human vein and microvascular endothelial cells. Effects of tumour necrosis factor alpha, interleukin 1 and phorbol ester. Biochem J 1993, 296:803–809
33. Maxwell AP, MacManus MP, Gardiner TA: Misonidazole binding in murine liver tissue: a marker for cellular hypoxia in vivo. Gastroenterology 1989, 97:1300–1303
34. Gross MW, Karbach U, Groebe K, Franko AJ, Mueller-Klieser W: Calibration of misonidazole labeling by simultaneous measurement of oxygen tension and labeling density in multicellular spheroids. Int J Cancer 1995, 61:567–573
35. Pournaras CJ, Riva CE, Tsacopoulos M, Strommer K: Diffusion of O2 in the retina of anesthetized miniature pigs in normoxia and hyperoxia. Exp Eye Res 1989, 49:347–360
36. Jiang BH, Semenza GL, Bauer C, Marti HH: Hypoxia-inducible factor 1 levels vary exponentially over a physiologically relevant range of O2 tension. Am J Physiol 1996, 271:C1172–C1180
37. Aiello LP, Pierce EA, Foley ED, Takagi H, Chen H, Riddle L, Ferrara N, King GL, Smith LE: Suppression of retinal neovascularization in vivo by inhibition of vascular endothelial growth factor (VEGF) using soluble VEGF-receptor chimeric proteins. Proc Natl Acad Sci USA 1995, 92:10457–10461
38. Nandgaonkar BN, Rotschild T, Yu K, Higgins RD: Indomethacin improves oxygen-induced retinopathy in the mouse. Pediatr Res 1999, 46:184–188
39. Yossuck P, Yan Y, Tadesse M, Higgins RD: Dexamethasone alters TNF-alpha expression in retinopathy. Mol Genet Metab 2001, 72: 164–167
40. Sharma J, Barr SM, Geng Y, Yun Y, Higgins RD: Ibuprofen improves oxygen-induced retinopathy in a mouse model. Curr Eye Res 2003, 27:309–314
41. Wilkinson-Berka JL, Alousis NS, Kelly DJ, Gilbert RE: COX-2 inhibition and retinal angiogenesis in a mouse model of retinopathy of prematurity. Invest Ophthalmol Vis Sci 2003, 44:974–979
42. Takahashi K, Saishin Y, Mori K, Ando A, Yamamoto S, Oshima Y, Nambu H, Melia MB, Bingaman DP, Campochiaro PA: Topical nepafenac inhibits ocular neovascularization. Invest Ophthalmol Vis Sci 2003, 44:409–415